

META MATERIALS COMPOSED OF COUPLED OSCILLATORS

THESIS

Submitted in partial fulfillment of the requirements of
BITS F421T, THESIS

K Pratyush Kumar
2016B5TS0435G

Under the supervision of
Dr. Shashi Thutupalli,
ICTS, TIFR



BITS PILANI, K K BIRLA GOA CAMPUS

Friday 6th December, 2019

Acknowledgements

I am profoundly grateful to Dr. Shashi Thutupalli for his expert guidance and continuous encouragement throughout to see that this project is true to its target.

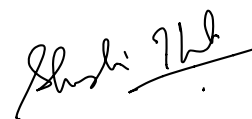
I would like to express my sincere thanks to Mr. Jyoti Prasad Banerjee for his valuable advice. Also, I would like to thank the members of The Thutupalli Lab who had assembled a setup which helped me develop my intuition for the project.

Words are insufficient to express my gratitude to my parents and my brother for their constant support during this project.

Finally, I would like to thank Hareesh, Pavan, Vibha, Rajat, Aditya, Misha, Raj, Siddharth and Toshi for their valuable inputs and company. Without the occasional chats and Star Wars nights, my thesis would not have been the same.

CERTIFICATE

This is to certify that the Thesis entitled, *Meta Materials composed of Coupled Oscillators* is submitted by *K Pratyush Kumar*, ID No. *2016B5TS0435G* in partial fulfillment of the requirements of **BITS F421T** Thesis embodies the work done by him under my supervision.



Signature of Supervisor

Name : Shashi Thutupalli
Designation : Reader, ICTS

Friday 6th December, 2019

List of Symbols and Abbreviations

The list describes several symbols and abbreviations that will be used in this Thesis

γ Drag or viscosity coefficient of medium

θ Phase angle

F Force between a pair of dipoles

h and dt Time step in numerical simulations

I Moment of inertia of rotor

m_i Dipole moment

T Active Center Period - time taken for a rotation by $\pi/3$

ACV Active Center Velocity

EOM Equations of Motion

Do... or do not. There is no try.
— *Yoda*,
The Empire Strikes Back, 1980.

Abstract

Meta materials, artificially synthesized and engineered materials have a wide range of applications. Such materials have been realized on honeycomb lattices. In this thesis we study such a potential meta material system for its wave propagation properties, particularly the existence of edge modes. The system is composed of six armed rotors coupled magnetically to each other on a honeycomb lattice; they exhibit oscillations, rotations or a combination of both depending on system parameters. Our results indicate that this model can not exhibit edge waves in its current configuration. The system exhibits rich collective behaviour and we study some of its properties such as kinetic energy propagation across the lattice and synchronization.

Contents

1	Introduction	3
1.1	System - Setup and EOM	3
2	Simulations - Algorithms and Implementation	5
2.1	Implementation	5
2.2	Algorithm - Velocity Verlet	6
2.3	Verification of the code	6
3	Relaxation Dynamics	8
3.1	Lattice - 97 Rotors	8
3.2	Two Rotor System	9
4	Active Central Rotor	13
4.1	Motivation	13
4.2	Investigation of Edge modes	13
4.3	Dynamical Systems perspective	15
4.3.1	Energy Distribution	15
4.3.2	Synchronization Patterns	18
4.4	Role of interaction forces	19
5	Conclusion	23
	Appendices	24
A	Perturbations on edge rotors	24
B	Parameter space - Non converging behaviour	26

Chapter 1

Introduction

Meta materials are materials that derive their properties from the geometry of the constituent elements and topology of the lattice rather than the chemical properties of the constituents. Meta materials have been developed in the past with properties such as negative refractive indices, or as cloaking devices amongst several other applications [3].

In this project we test the wave propagation properties of a system of rotors coupled by magnetic dipoles placed on their edges on a honeycomb lattice. Honeycomb lattices have been shown to exhibit edge waves [4] and magnetic rotors with six-fold symmetry have also been studied[6]. The system is interesting in its own right as a complex system, and hence we investigate it for interesting collective behaviour. An experimental setup was assembled by members of the Thutupalli lab at NCBS, Bengaluru. We use this setup for verifying the equilibrium configuration from simulation.

1.1 System - Setup and EOM

We use a rotor composed of six spokes - with a magnetic dipole placed at the end of each spoke, this design was inspired by [6]. The dipoles are placed such that all of them face outward, Fig. 1.1. These rotors are placed on a honeycomb lattice. The system also includes dissipation due to drag forces. There are two forces in play here - the interaction force which leads to a torque on the rotors and a velocity dependent torque for dissipation.

The force between two dipoles[2] is given as follows :

$$\vec{F} = \frac{1}{r^5}(\vec{r}(\vec{m}_a \cdot \vec{m}_b) + \vec{m}_a(\vec{r} \cdot \vec{m}_b) + \vec{m}_b(\vec{r} \cdot \vec{m}_a)) - \frac{5\vec{r}}{r^7}(\vec{r} \cdot \vec{m}_a)(\vec{r} \cdot \vec{m}_b)$$

where \vec{r} is the vector joining the two dipoles, and m_a and m_b are the dipole moments.

The equation of motion is :

$$I\ddot{\theta}_i = -\gamma\dot{\theta}_i + \sum_{\{i,j\}} \sum_{m=1}^{m=6} \sum_{n=1}^{n=6} \vec{r}_i^m \times \vec{F}^{mn}$$

where I is the moment of inertia of rotors, θ is the angle of rotor w.r.t the X axis. Since the rotor has a six fold symmetry, the angle can be specified by any arm. We select an arbitrary arm and use it to specify the position. γ is the drag coefficient of the medium. \vec{r}_i^m is the vector joining the axis of the m^{th} rotor to the i^{th} dipole on it. F^{mn} is the force between two dipoles.

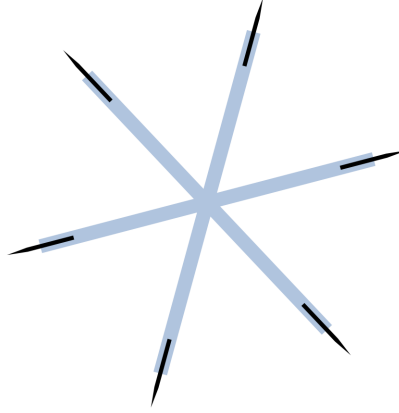


Figure 1.1: Illustration of a rotor with dipoles(black). The center of the dipoles are on the end of the rotor arm.

Now we place the rotors on a lattice. A honeycomb lattice is generated by repeating hexagons on a 2D plane as shown in Fig.1.2. Note that this is not a Bravais lattice.

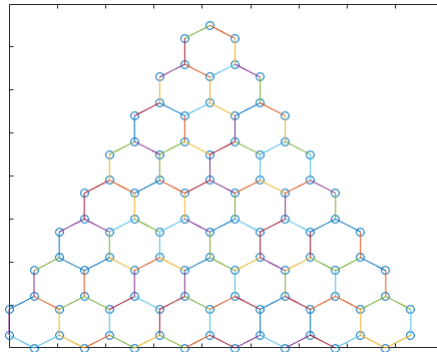


Figure 1.2: A honey comb lattice with 97 sites. The lines joining the sites represent nearest neighbor links.

The electrostatic force is a long range force, but to save computational time we need to impose a cut off. We restrict the interaction to nearest neighbors. As is evident from the EOM and the interaction force, a direct analytical solution is not viable so we investigate the system computationally.

Chapter 2

Simulations - Algorithms and Implementation

In molecular dynamics simulations, the forces on each molecule are computed and the trajectory is determined accordingly, often for a very large number of molecules. Since we have multiple coupled 2nd order ODEs, we can use techniques from molecular dynamics. We use an algorithm called Velocity Verlet [5] which is a symplectic integrator. Symplectic integrators are integration schemes that are designed to conserve the energy of the system up to a numerical error. In Runge-Kutta schemes, we know that the total energy of a conservative system varies monotonically with time. However for a symplectic integrator, the total energy keeps fluctuating about its actual value. In the absence of friction, conservation of energy can be used as a good test of whether we are capturing the physics of the system correctly. However there is a downside to these algorithms; the trajectory in phase space is not as accurate as RK schemes and deviates faster from the true solution.

2.1 Implementation

The simulation is written in MATLAB and implemented in the following manner :

1. The spatial coordinates of a single hexagon are hard coded.
2. The hexagon is repeated as many times as required.
3. An adjacency matrix is constructed by calculating the distance between each pair of sites. This can be used to save computational time during force calculations.
4. We construct loops that go over each pair of sites and check if they are neighbors using the matrix. The forces and torques are computed for each dipole pair across the two rotors.
5. The Velocity Verlet algorithm is used to calculate the solution. Details in section 2.2.

2.2 Algorithm - Velocity Verlet

Velocity Verlet is a 2nd order symplectic integrator[5] which is a commonly used method in molecular dynamics due to its simplicity and computational speed. Since our system has dissipation the Hamiltonian is not conserved and the algorithm in its original form is not usable. We use a variant of the algorithm which takes into account drag effect. Clearly, the energy is not conserved with this variant. For an ODE of the form $m\ddot{x} = f(x, t)$, and with time step as h

$$x(t + h) = x(t) + v(t)h + \frac{f(t)}{2m}h^2 \quad (2.1)$$

$$v(t + h) = v(t) + \frac{h}{2m}[f(t) + f(t + h)] \quad (2.2)$$

$$(2.3)$$

It can be shown that the error in position is of the order 4, while in velocity it is order 2. The algorithm is invariant under time reversal ($h \rightarrow -h$). Time reversibility is important for conservation laws, and symplectic integrators like these conserve a pseudo Hamiltonian which varies from the actual Hamiltonian by a small amount. The error goes to zero as $h \rightarrow 0$. The drag variant, for an ODE of the form $m\ddot{x} = f(x, t) - \gamma v$:

$$x(t + h) = x(t) + v(t)h + \frac{1}{2}h^2a(t); \quad a(t) = \frac{f(x, t) - \gamma v}{m} \quad (2.4)$$

$$v(t + h) = \frac{1}{1 + h\gamma/2m}[v(t)(1 - h\gamma/2m) + \frac{h}{2m}(f(t) + f(t + h))] \quad (2.5)$$

2.3 Verification of the code

To check if the written code was functioning correctly, the following checks were performed :

1. The force and torque values were computed analytically for two dipoles in specific positions and matched with force and torque given by the code.
2. A single rotor was given an initial velocity and its velocity was plotted w.r.t time. As expected the velocity decayed exponentially $\sim \exp(-2\gamma/I)$
3. Multiple (97) rotors were started of with random phases and velocities but the force was scaled down by a factor of 1e-4. And the kinetic energy decayed as expected $\sim \exp(-2\gamma/I)$
4. Without friction - Two rotors with one dipole each were oriented such that the dipoles point away from each other. They were initialized with small and equal perturbations in their phase. We would expect them to undergo periodic motion under small oscillation approximation and they exhibit that behaviour as expected. In the presence of friction, the oscillations decay exponentially.
5. In presence of friction, two rotors each with six dipoles initialized with random phases and velocities eventually come to rest in a minima of the potential. This equilibrium orientation matches experimentally observed equilibrium, Fig. 2.1

6. The algorithm used is an energy conserving algorithm and hence the conservation of energy itself is a good test. In absence of friction, the energy is conserved.

A similar code in C was written. However there was a stark difference in the solution obtained. The C code was deemed faulty as it violated energy conservation. After multiple attempts at debugging, the fault could not be spotted. In presence of friction the equilibrium configuration is identical but the trajectory is different for the two codes. The nature of the error in the solution indicates that it is a numerical or precision error rather than a coding error. However, a concrete explanation is still required.

In our simulations we encountered aperiodic behaviour for certain parameters. We check the solution convergence by decreasing the time step, in certain cases it converges to a periodic solution. This is further discussed in Appendix B.



Figure 2.1: Equilibrium configuration

Chapter 3

Relaxation Dynamics

In this chapter we present the results for a lattice as well as a two rotor sytem.

3.1 Lattice - 97 Rotors

We investigate the relaxation dynamics of a system of 97 rotors started with random initial positions and velocities and we study how they come to rest. We observe exponential decays with two different slopes. This was determined by fitting $\ln(KE)$ to a straight line. In the initial times, we see a significant deviation of the fit from the data. In the regions where the error was significant, the data was fit to a line with a different slope. We explain this behaviour further in the next section. In the figures below the red line depicts the fit for the entire data while the purple line is the fit better suited to early time.

In the next section we study this transition with two rotors.

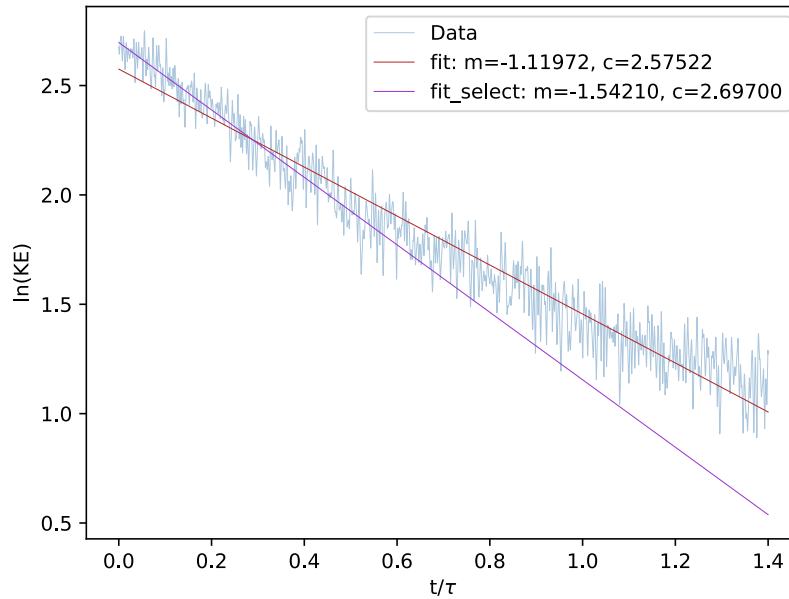


Figure 3.1: Decay of Kinetic Energy for 97 rotors. $\gamma = 0.0056$.

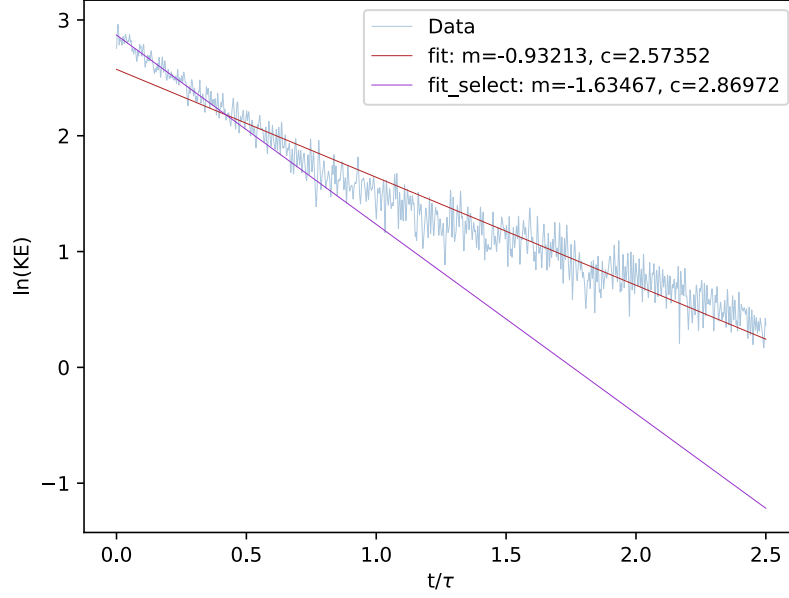


Figure 3.2: Decay of Kinetic Energy for 97 rotors. $\gamma = 0.01$.

3.2 Two Rotor System

We saw in the previous section that there are two types of decay in the system. To better understand this phenomena, we study a system of two rotors and get some interesting results. We restrict the motion of one rotor by holding it at rest and the other rotor is initialized with some velocity and allowed to relax to equilibrium. As evident from Fig. 3.3 there are two types of decay with a transient in between. We fit the initial and final parts to a straight line to obtain the exponent for the decay. In the initial time, the decay of Kinetic energy $\sim \exp(-2t/\tau)$ where $\tau = 1/\gamma$ is the same as non interacting rotor. At later times, it becomes $\exp(-t/\tau)$. We see there is a cutoff Kinetic Energy below which the interaction kicks in.

Our explanation is the following: The interaction torque acting on the rotors arises from magneto-static forces. These forces are dependent solely on the position and orientation of dipoles. The torque will not be influenced by the velocity of the rotor. Therefore the only parameter that can cause changes in the trajectory is the time duration for which the torque acts. At higher velocities, this time is very less. This explains the decay in kinetic energy, almost as if there are no interaction forces at higher velocities.

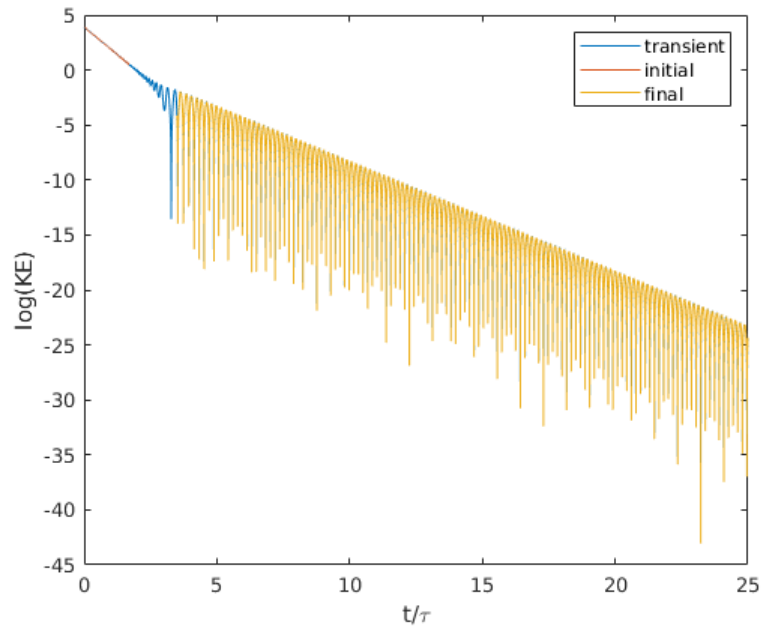


Figure 3.3: Decay of Kinetic Energy for two rotors (one rotor fixed) with $\gamma = 0.1$. Two types of decay are clearly visible.

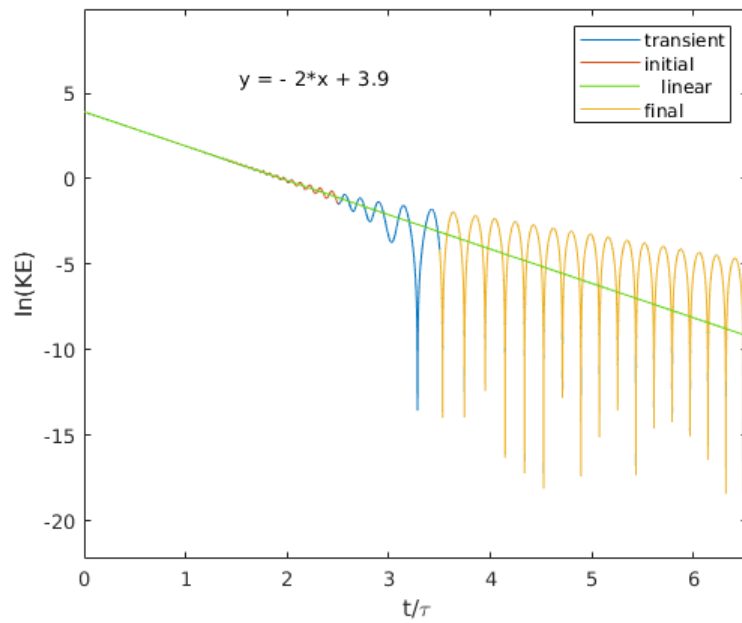


Figure 3.4: Decay of Kinetic Energy for two rotors (one rotor fixed) with $\gamma = 0.1$. The initial part of the data is fitted to obtain an exponent of 2

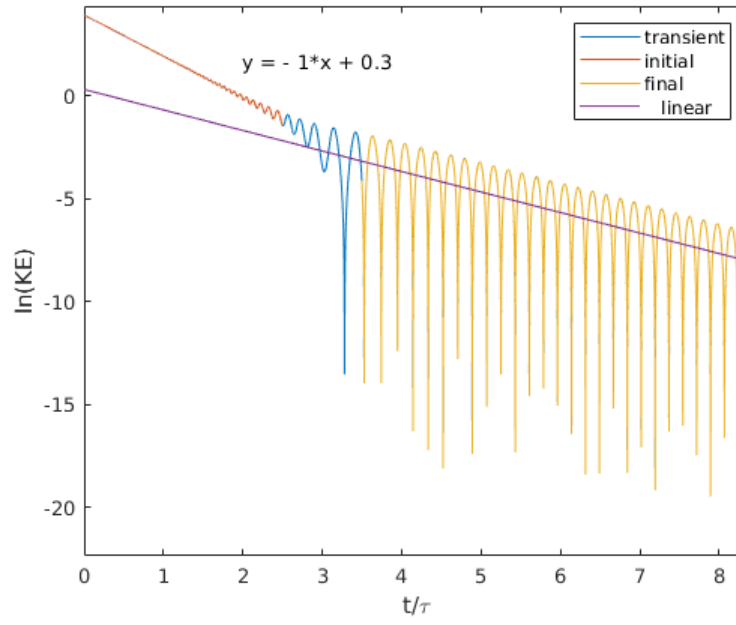


Figure 3.5: Decay of Kinetic Energy for two rotors, (one rotor fixed) with $\gamma = 0.1$. The final part of the data is fitted to obtain an exponent of 1

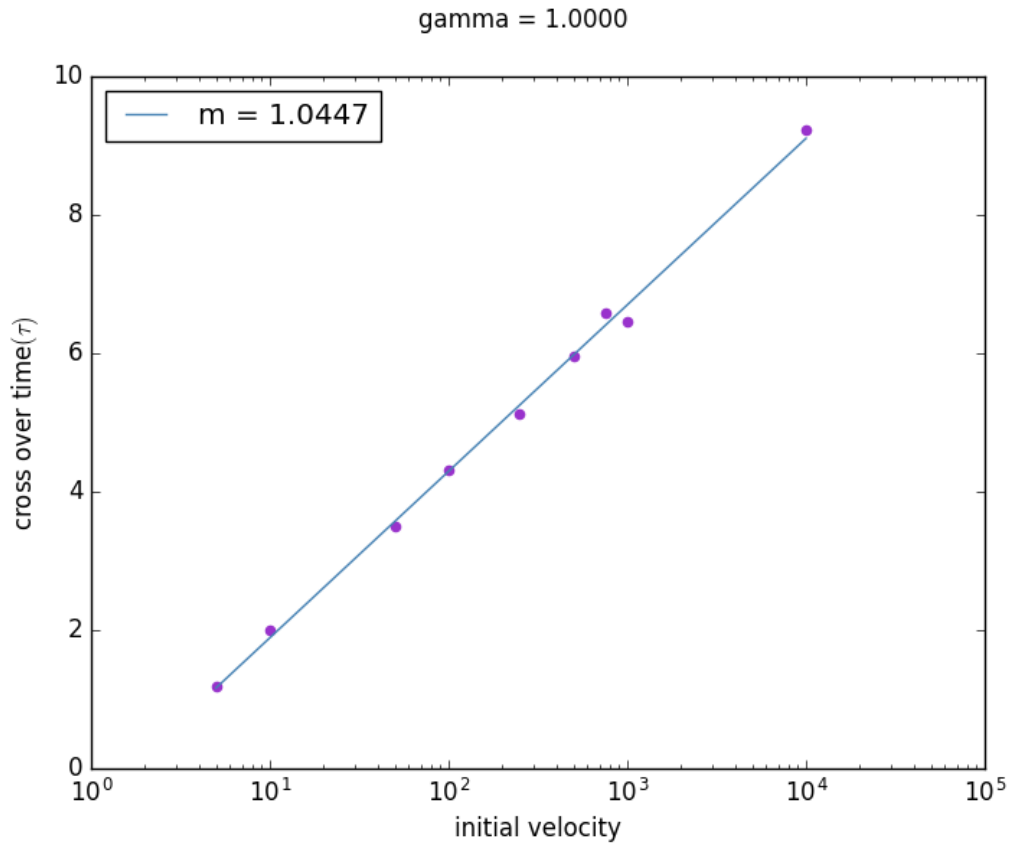


Figure 3.6: Cross over time vs. v_0 . This simulation result matches with the analytical calculation.

The crossover time varies as the log of initial velocity of the rotor (Fig. 3.6), this can also be derived analytically. At crossover time t_c , the kinetic energy is K_c .

$$K = K_0 \exp(-2t/\tau) \quad (3.1)$$

$$K_c = K_o \exp(-2t_c/\tau) \quad (3.2)$$

$$\frac{t_c}{\tau} = \log(v_0/v_c) \quad (3.3)$$

Chapter 4

Active Central Rotor

In this chapter, we investigate how the system behaves when energy is being pumped into the system via an active central rotor.

4.1 Motivation

It has been shown that gyroscopes coupled with magnetic forces can exhibit edge waves at certain frequencies on a honeycomb lattice [4]. By adding an active center we expect the rotors in the bulk to be influenced by the center, while those near and at the edges to be less influenced. *Our hypothesis is that a perturbation on the edge will travel only along the edge and not through the bulk.* The motivation behind this hypothesis comes from the interplay of broken time reversal symmetry and the lattice topology [4].

4.2 Investigation of Edge modes

The rotor in the centroid of the lattice is rotated with a constant velocity - we call this an active center. The active center can not react to any other rotor in the lattice, but other rotors in the lattice react to the active center. We try this for different velocities. The initial positions for the rotors are obtained from the equilibrium configurations from the relaxation study in Chapter 3. It is observed that half of the rotors rotate in clock wise direction while the other half rotates in the anti clock wise direction. The two parameters in the system are the ACV (Active Center Velocity) and γ . Both parameters lend us two different time scales. We see different kinds of behaviour as we vary these parameters. For high active velocities (time scale from active velocity is very less compared to the $\tau = 1/\gamma$) we see that the rotors exhibit oscillations and energy is not propagated from the center to the edge effectively which will be explained in further sections. The main objective of the study was to determine if the lattice can exhibit edge waves. To investigate this, we use two methods :

1. In the parameter space, we focus on the regions where rotors at the edge are not influenced by the active center. Perturbations are introduced on the edge to see if they travel through the bulk or edge.
2. A more reliable way of answering this question is to get the power spectrum of each rotor in its steady state. We can compare the power spectra of bulk

rotors with that of the edge rotors; if we see any frequencies present in the edge spectra that are absent in the bulk, we can conclude that edge modes are present.

We did the first analysis for a few parameters but did not observe edge waves. This method is inconclusive and not exhaustive because we do not know which frequencies and amplitudes can lead to edge waves. The results are given in Appendix A.

Using the second method, we find that there are no extra frequencies in the edge spectra; representative plots are shown in Fig. 4.1. Hence we conclude that no edge waves are being exhibited by the system in its current configuration. However in Fig. 4.1a, we see that there are certain frequencies present in the bulk spectra which are not present in the edge spectra. This observation needs to be investigated further.

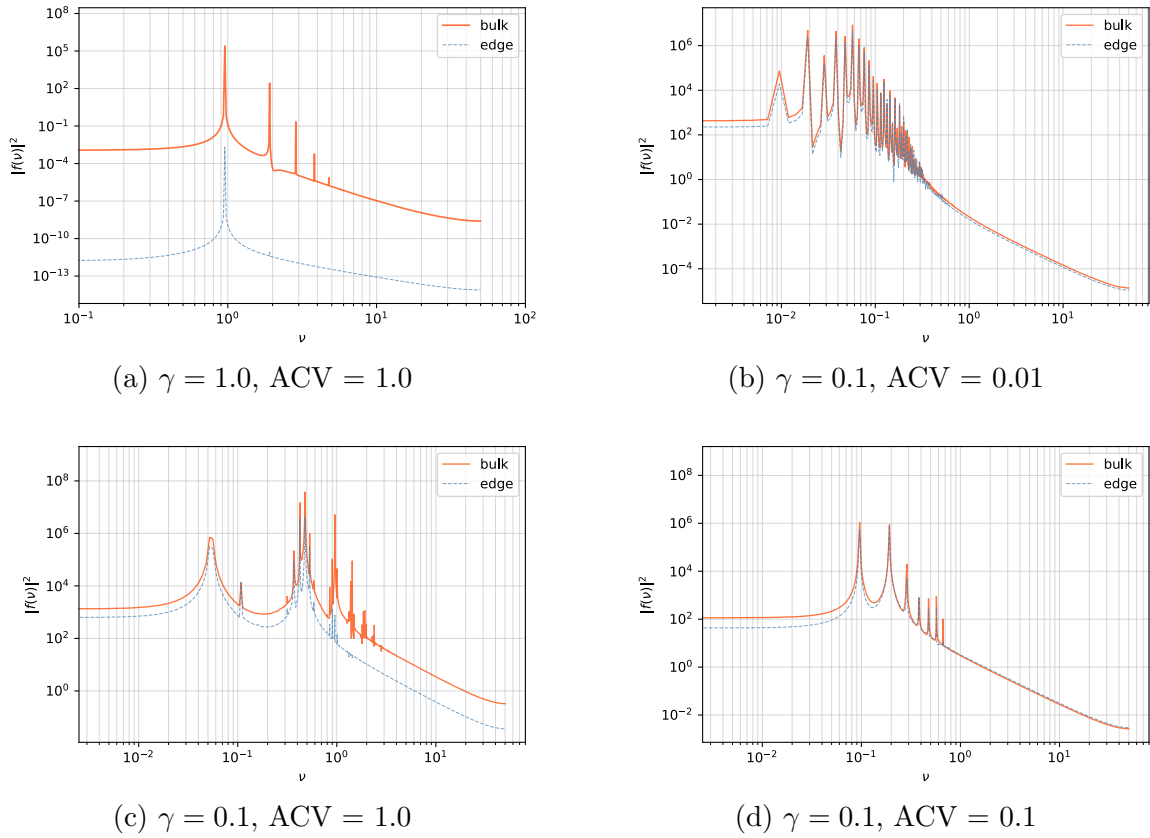


Figure 4.1: Power spectra : Power spectrum is computed for each rotor and then bulk (edge) spectrum is obtained by adding the spectra of all the bulk (edge) rotors. The edge spectra does not show any extra frequencies.

4.3 Dynamical Systems perspective

A single rotor placed in a dissipative medium will eventually come to rest with an exponential decay, but when multiple rotors are present, we see interesting dynamics as described in Chapter 3. In addition to this, when we added an active rotor, the dynamics became very complex and it becomes worthwhile to study it from a nonlinear dynamics perspective.

There are four interesting aspects that we notice :

1. As evident from figures 4.7, 4.8 and 4.9, the phases exhibit different types of behaviour like oscillations, rotations and a combination of both.
2. The system settles into a steady state and the energy distribution among the rotors shows a transition as γ and ACV are varied. Fig. 4.5
3. The rotors show synchrony patterns.
4. Interaction potential and lattice specifications play an important role in the dynamics of the system.

4.3.1 Energy Distribution

For most of parameter space, the system settles into a steady state periodic motion after some time, depending on the time scales. The time scale from ACV i.e. the period of rotation by $\frac{\pi}{3}$ is denoted by T . The characteristic time obtained from the drag coefficient is γ . The Kinetic energy shows a variety of behaviours, which can be broadly classified as :

1. $\tau \gg T$, Periodic excitation and relaxation, with an exponential decay envelope.
2. $\tau \approx T$, Either aperiodic behaviour or oscillations about a non-zero value.
3. $\tau \ll T$, Periodic excitation and relaxation.

In Fig. 4.2 and 4.4, it can be seen that the kinetic energy is highest at the edge. Further, the rotors across the lattice have a high kinetic energy at the same instants of time. However, Fig. 4.3 shows a spatio-temporal wave. At $t \approx 18.1$ a pulse can be seen at $r = 3.0$, tracking this pulse forward in time we see that it reaches the edge at $t \approx 18.6$ and gets reflected back.

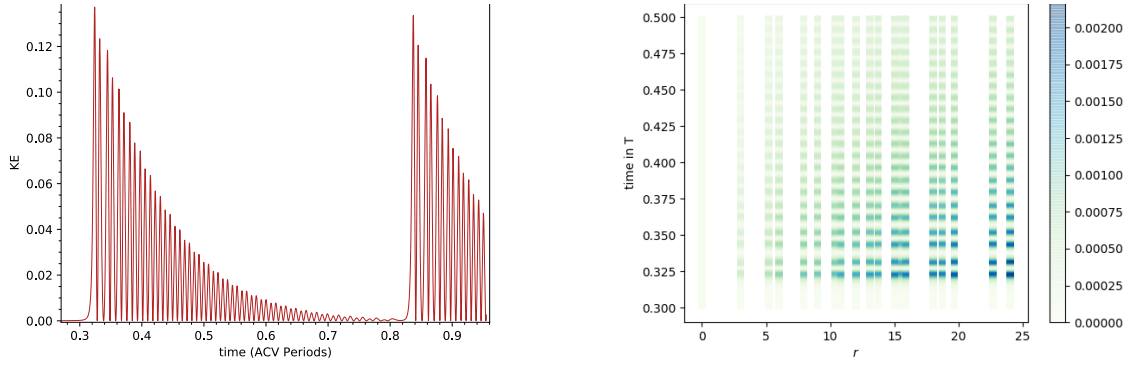


Figure 4.2: $\gamma = 0.01$, $\text{ACV} = 0.001$, $T = 1047.2$ s. Oscillations with exponential envelope and standing waves.

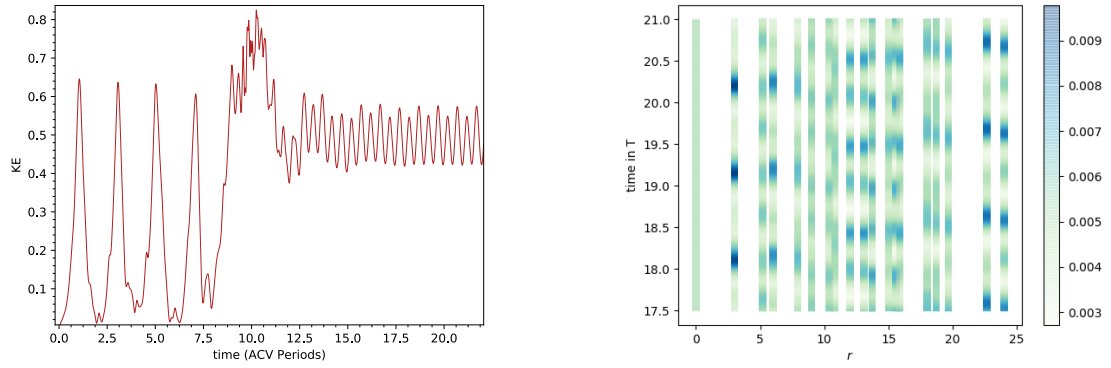


Figure 4.3: $\gamma = 0.1$, $\text{ACV} = 0.1$, $T = 10.47$ s. Oscillations about mean non zero energy. The plot on the right shows the energy pulse travelling from the center to edge and getting reflected.

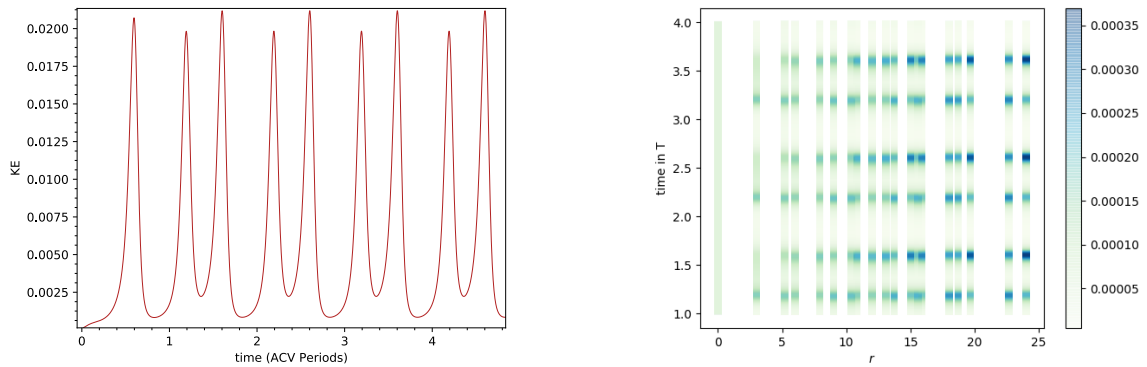


Figure 4.4: $\gamma = 1.0$, $\text{ACV} = 0.01$, $T = 104.72$ s. Periodic excitation and relaxation with standing waves

The distribution of energy over the rotors is also interesting since it shows a 'transition'. To investigate this we find the average kinetic energy of each rotor, over a sufficient time period. Edge rotors are defined to be those with only two neighbours. We observe three types of distributions :

1. Energy of edge rotors is the highest, and it decreases as we move to the center of the lattice. This is observed for low ACVs.
2. Energy of the center is the highest and decreases as we move to the edge. This is observed for high ACVs. In certain cases, the kinetic energy shows a local minima.
3. Uniform distribution of energy; edge, bulk and central rotors have the same energy.

To better understand this, we plot the time averaged kinetic energy as a function of radial distance in Fig. 4.5. The behaviour of the curves change with ACV.

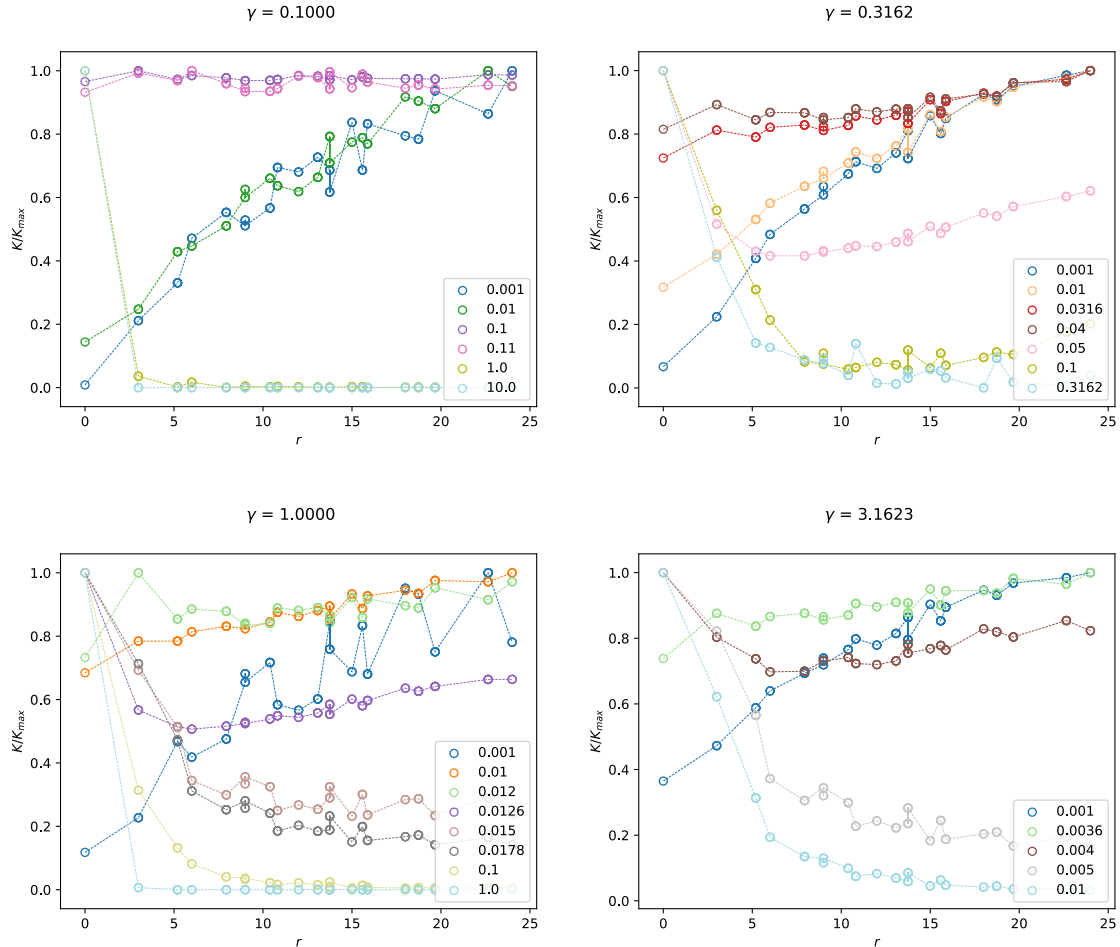


Figure 4.5: Time averaged kinetic energy vs. radial distance, the average is taken over a few periods. The index shows different ACVs. For each active velocity, we normalize the kinetic energy values by the maximum so that we can see the transition happening clearly.

At low ACVs, the kinetic energy is getting transferred to the rest of the lattice effectively while at higher ACVs the kinetic energy gets confined up to a certain radius; this follows from the phenomena explained in Chapter 3. We present a rough phase diagram for the system in Fig. 4.6. In the spread phase the kinetic energy is propagated through out the lattice, while in the restricted phase it is restricted to the central region.

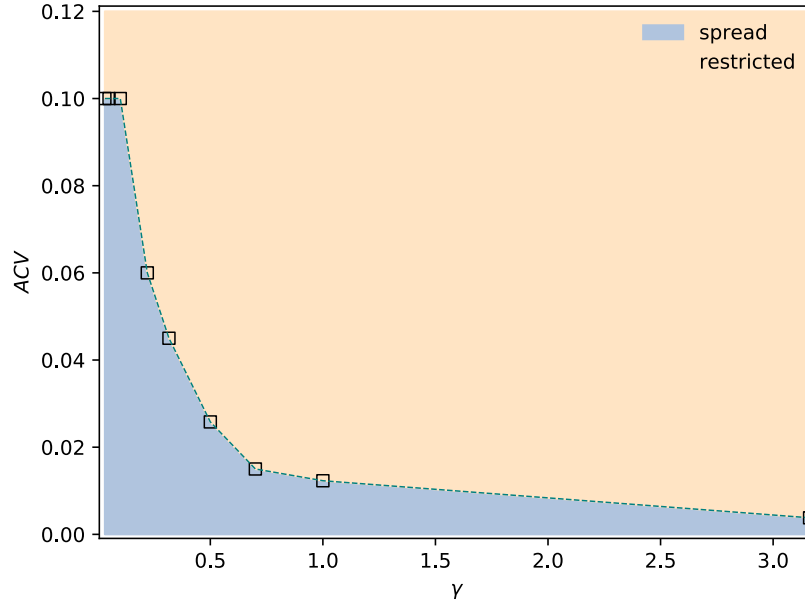


Figure 4.6: Phase diagram showing the two types of energy propagation.

4.3.2 Synchronization Patterns

The rotors have a six fold symmetry, therefore the relevant phase is from zero to $\pi/3$. An order parameter similar to the Kuramoto order parameter[1] can be defined which measures if the rotors are pointing in the same direction : $\sum \exp(in\theta)$, where n is number of arms. We can see in Fig. 4.7, 4.8, 4.9 that there is a clustering of phases, i.e there are clusters of rotors which are synchronized. We see two distinct clusters with opposite velocities, further focusing on these clusters reveal that they are clustered with almost perfect synchrony.

Phase oscillators like Kuramoto oscillator [1] exhibit synchronization, and this behaviour is subject to the network characteristics. We would therefore, expect that existence of synchronized clusters is also a consequence of the lattice properties. By identifying the clusters on the lattice we observe that these clusters are formed at fixed radii. Fig. 4.10

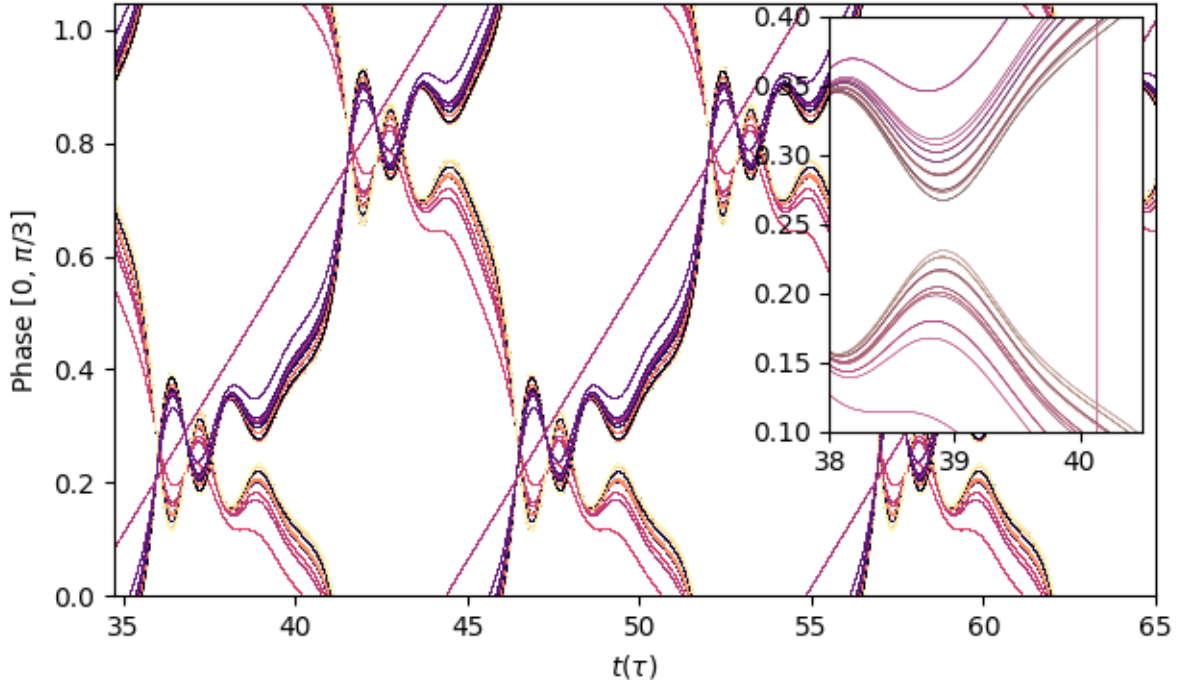


Figure 4.7: $\gamma = 0.1$, $ACV = 0.01$, $N = 97$. Patterns periodic in time are observed in the phases of all 97 rotors, the inset shows clusters of synchronized rotors. The synchronized clusters can further be classified into two large clusters. In each of the large clusters, rotors are partially synchronized.

4.4 Role of interaction forces

It has been shown previously that honeycomb lattices show properties like edge modes [4]. Although we have not seen edge waves in our lattice, we see other kinds of properties like waves propagating through the bulk and reflections at the edge, standing waves, and synchronization. It is an interesting question to ask if these are a result of the lattice geometry or due to the magnetic dipole interactions? This can be studied by simulating for an r^6 repulsive potential instead of magnetic dipoles. We observe that the dynamics are very different from the original system. The rotors away from the center, do not show any kind of motion and the rotors close to the active center exhibit oscillations about their mean position, Fig. 4.11 and Fig. 4.12.

Hence, we conclude that the lattice geometry and the magento-static interaction, both play an important role in these dynamics.

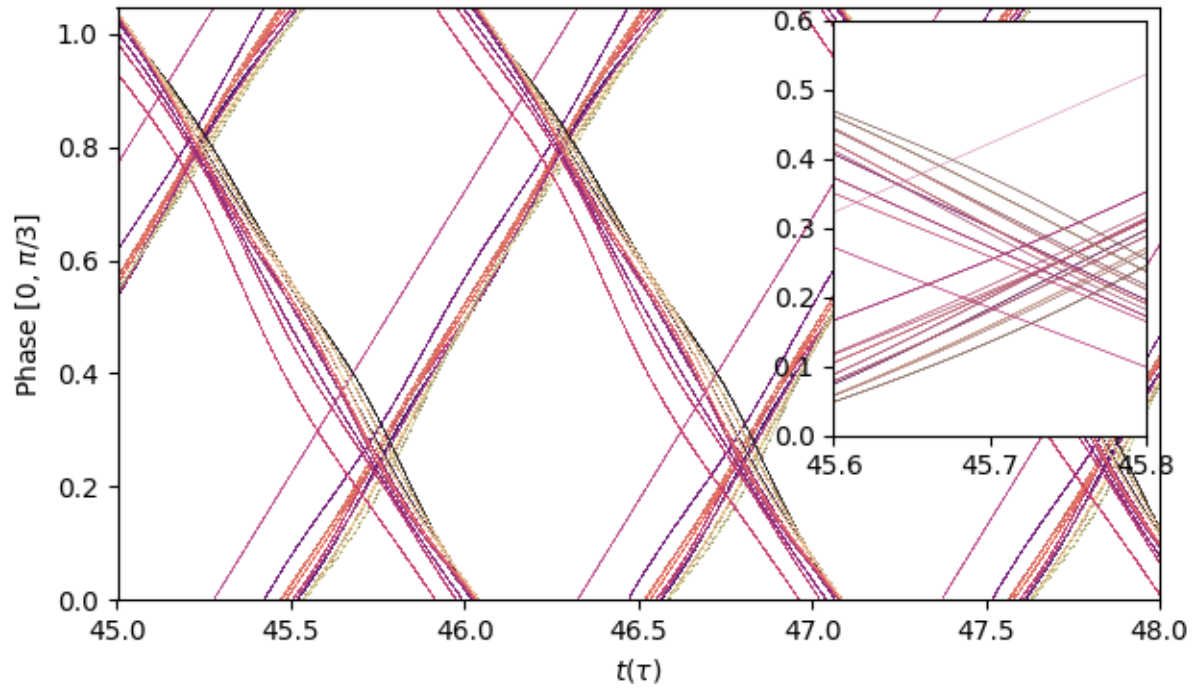


Figure 4.8: $\gamma = 0.1$, $ACV = 0.1$, $N = 97$. The rotors are spinning continuously and do not change their direction. Inset shows clusters.

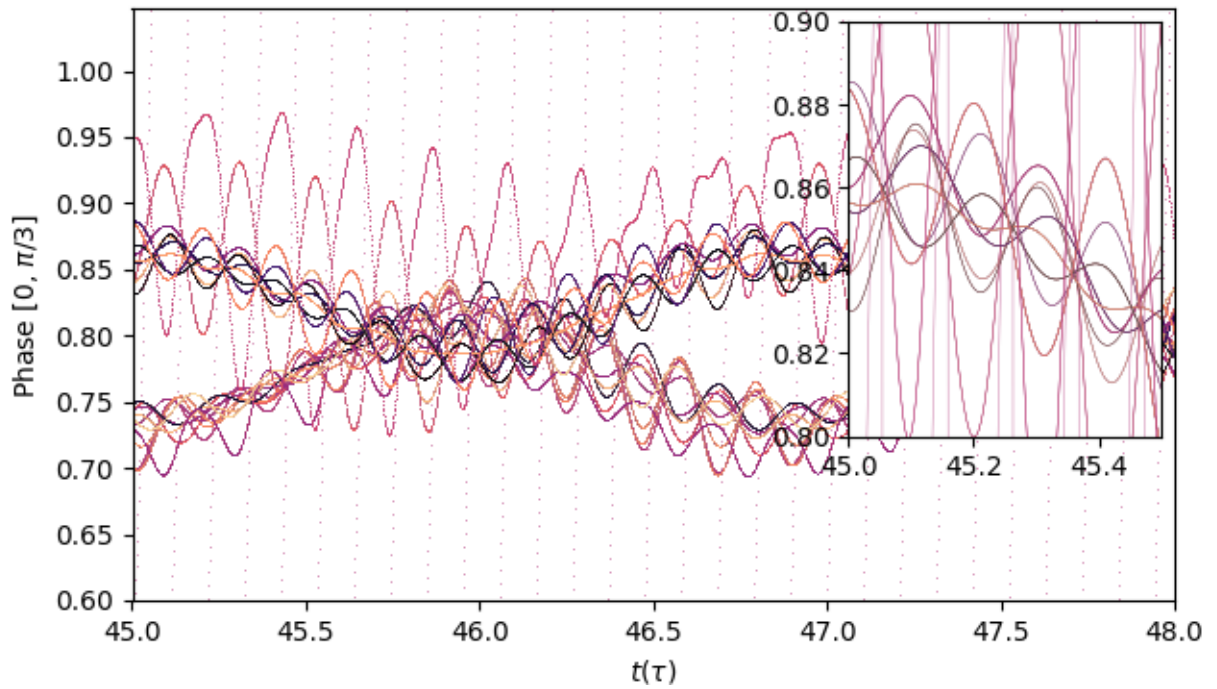


Figure 4.9: $\gamma = 0.1$, $ACV = 1.0$, $N = 97$. The rotors oscillate about their equilibrium positions, instead of spinning continuously.

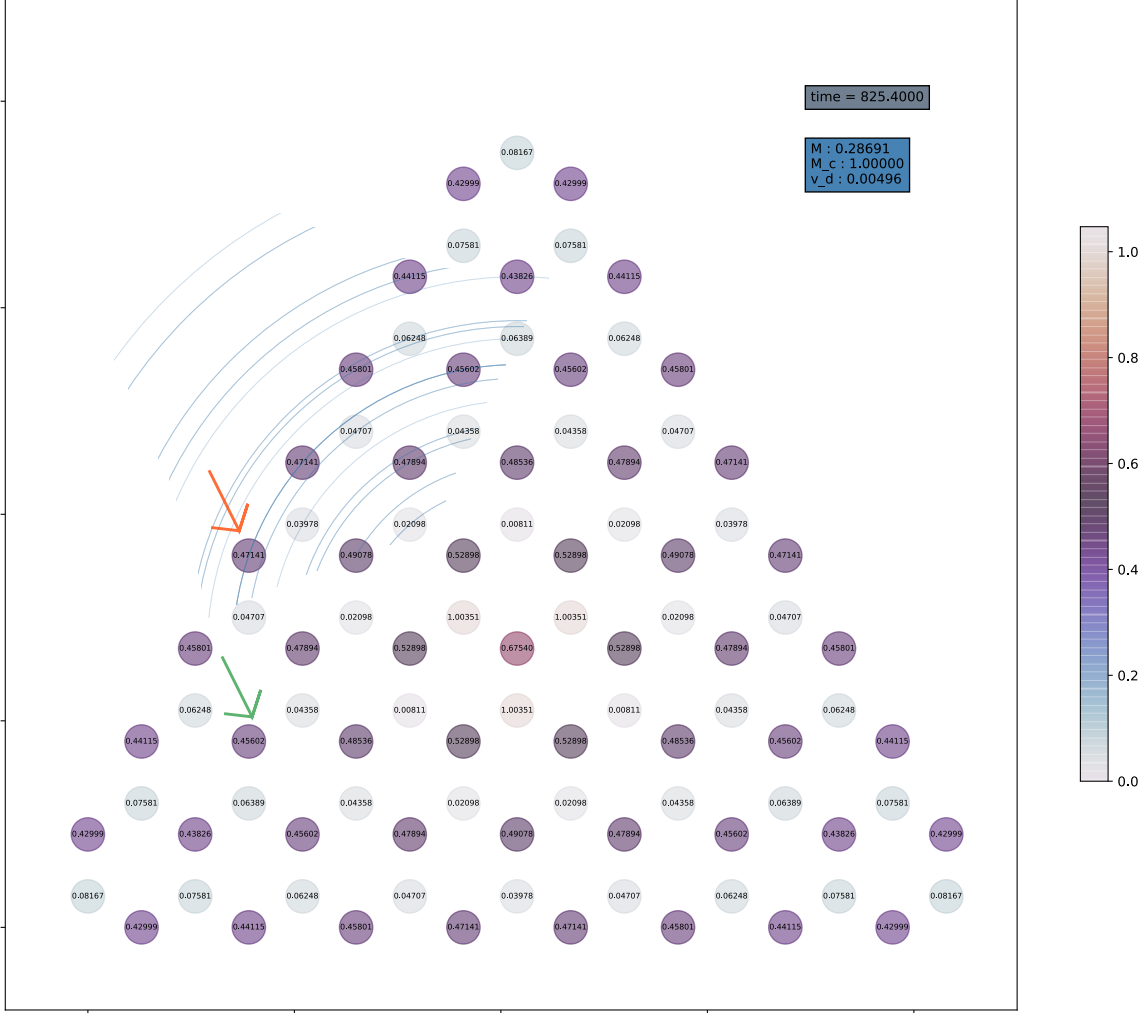


Figure 4.10: $\gamma = 0.1$, $ACV = 0.01$, $N = 97$. The smaller solid circles represent rotors. The color of the circle indicates the phase in radians, which is also written inside the circle. The faint circles represent clusters at fixed radii. The green and orange arrows show the rotors which are on the same circle, but show different phases. This maybe caused by the boundary effects. M and M_c are the order parameter for the entire lattice and average over absolute value of cluster order parameters respectively. v_d is the dispersion in velocities.

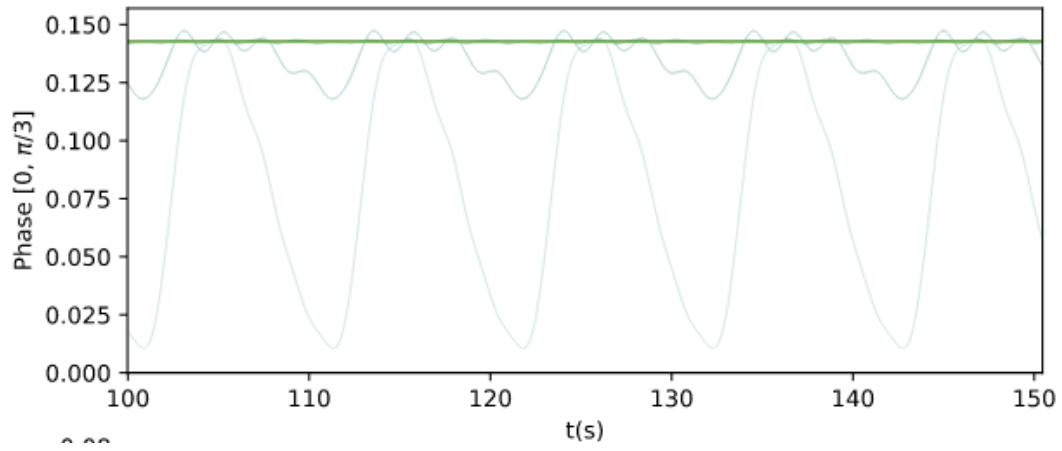


Figure 4.11: $\gamma = 0.1$, $ACV = 0.1$

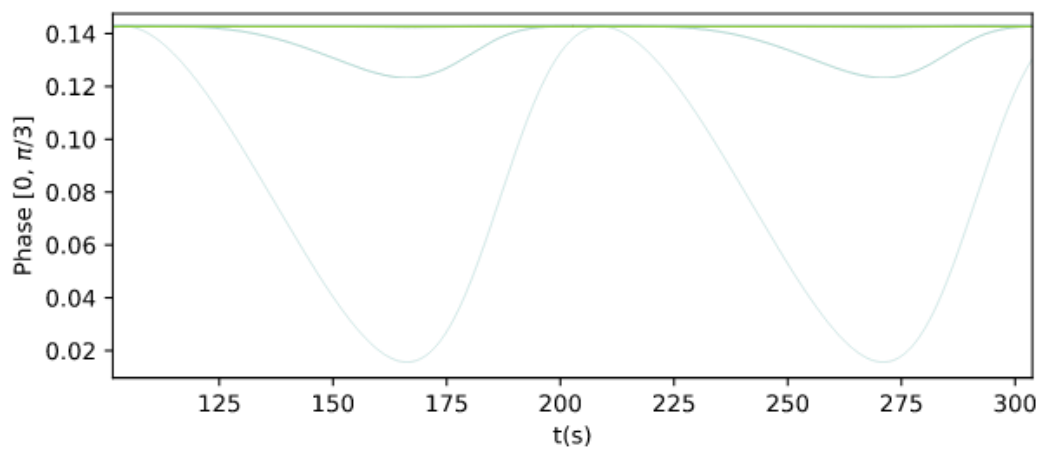


Figure 4.12: $\gamma = 0.1$, $ACV = 0.01$

Chapter 5

Conclusion

We have shown that rotors with six fold symmetry and magnetic coupling on a honeycomb lattice with active centre, do not exhibit edge waves by studying the power spectra and by introducing perturbations. In this process, however, we have uncovered several interesting phenomena that this system is capable of exhibiting : travelling waves, standing waves and synchronized clusters. This system in its current state may not serve as a viable meta material; but owing to the large number of interacting entities, it can show other interesting dynamical behaviour which we may have missed. One interesting aspect that can be explored is the role of symmetry in the rotor i.e. how a rotor with an n -fold symmetry will behave on this lattice. Even though we do not see waves on the edge, we do see frequencies in the power spectra of the bulk that we do not see in the edge. Although this is not what we expected, this result gives us a direction to proceed for studying this system.

Appendix A

Perturbations on edge rotors

The system with active an rotor is allowed to reach a steady state. We select those system parameters for which the the rotors away from the center are not influenced heavily by the active rotor. One such parameter is $\gamma = 1.0$ and $ACV = 0.1$, for which we show the analysis and results.

Once, the system has reached steady state, we select a rotor on the edge of the lattice and rotate it with a constant velocity for at least one period T . Then we check whether the energy from this perturbation travels along the edge or through the bulk. This can be done by making an animation of the lattice, where the color of the site represents kinetic energy. The other way is to plot figures like Fig. 4.2. These plots are presented below in Fig. A.1 and A.2. This method is not exhaustive since we can try many different velocities and duration of perturbations. However, the power spectra analysis that we performed is a reliable method to conclude that edge waves are not present.

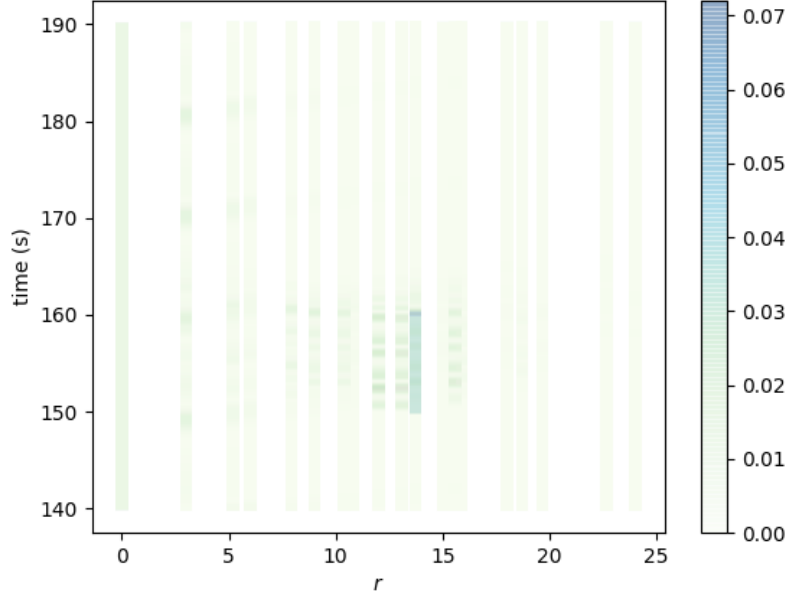


Figure A.1: $\gamma = 1.0$, $ACV = 0.1$, $PV = 0.3$, $\delta t = 10s$. PV is the perturbed rotor's velocity and δt is duration of the perturbation, perturbation starts at $t = 150$. The perturbation can be seen as the dark stretch at $r \approx 13$, it is observed that the energy travels inside, rather than propagating on the edge.

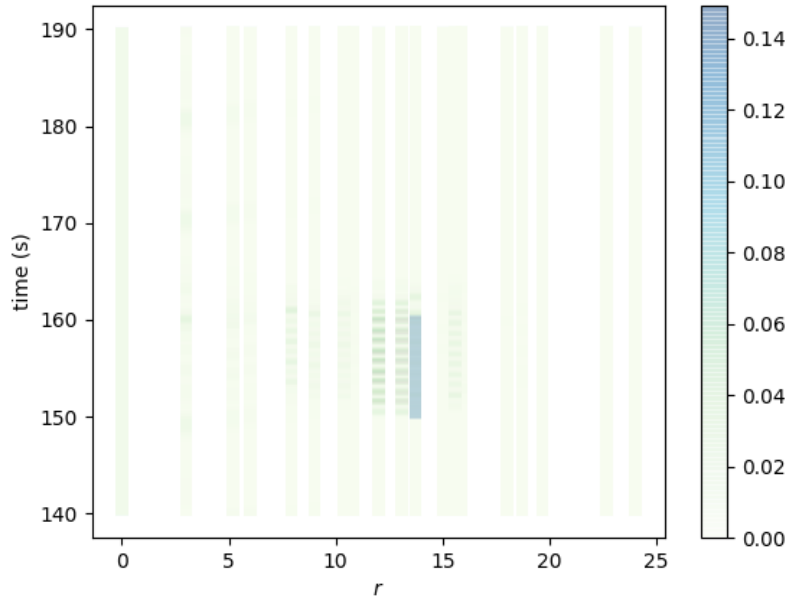


Figure A.2: $\gamma = 1.0$, $ACV = 0.1$, $PV = 0.5$, $\delta t = 10s$. PV is the perturbed rotor's velocity and δt is duration of the perturbation, perturbation starts at $t = 150$. The perturbation can be seen as the dark stretch at $r \approx 13$, it is observed that the energy travels inside, rather than propagating on the edge.

Parameter space - Non converging behaviour

In our simulations we have encountered certain system parameters where we encounter aperiodic behaviour. To investigate this we decrease our time step and check for convergence. This analysis is summarised below :

[illegible]

The interpolated region is where we have not simulated the system but we do not expect aperiodic behaviour. In the white region we have not done simulations but there might be aperiodic behaviour there.

Bibliography

- [1] Juan A. Acebrón et al. “The Kuramoto model: A simple paradigm for synchronization phenomena”. In: *Rev. Mod. Phys.* 77 (1 Apr. 2005), pp. 137–185. DOI: 10.1103/RevModPhys.77.137. URL: <https://link.aps.org/doi/10.1103/RevModPhys.77.137>.
- [2] Peter B. Landecker, Daniel D. Villani, and Kar W. Torrance Yung. “AN ANALYTIC SOLUTION FOR THE TORQUE BETWEEN TWO MAGNETIC DIPOLES”. In: 1999.
- [3] *Metamaterials*. 2010. URL: <https://www.sciencedirect.com/topics/materials-science/metamaterials>.
- [4] Lisa M. Nash et al. “Topological mechanics of gyroscopic metamaterials”. In: *Proceedings of the National Academy of Sciences* 112.47 (Nov. 2015), pp. 14495–14500. ISSN: 1091-6490. DOI: 10.1073/pnas.1507413112. URL: <http://dx.doi.org/10.1073/pnas.1507413112>.
- [5] Anders Sandvik. *Numerical Solutions of Classical Equations of Motion*. 2018. URL: <http://physics.bu.edu/py502/lectures3/cmotion.pdf>.
- [6] Javier Vila, Glaucio H. Paulino, and Massimo Ruzzene. “Role of nonlinearities in topological protection: Testing magnetically coupled fidget spinners”. In: *Physical Review B* 99.12 (Mar. 2019). ISSN: 2469-9969. DOI: 10.1103/physrevb.99.125116. URL: <http://dx.doi.org/10.1103/PhysRevB.99.125116>.